



Journal Name

ARTICLE

Preparation and characterization of terdentate [C,N,N] acetophenone and acetylpyridine hydrazone platinumacycles. A DFT insight into the reaction mechanism

Received 00th January 20xx,
Accepted 00th January 20xx

DOI: 10.1039/C7DT03418K

www.rsc.org/

Ismael Marcos,^a Vicente Ojea,^a Digna Vázquez-García,^{a*} Jesús J. Fernández,^a Alberto Fernández,^a Margarita López-Torres,^a Jorge Lado^a and José M. Vila.^{b*}

Reaction of *N-orto*-chlorophenyl substituted acetylpyridine hydrazones (**a** and **d**) with K₂[PtCl₄] (*n*-butanol/water, 100 °C) gave mononuclear complexes **1a** and **1d** with the ligands as [N,N] bidentate. Contrastingly, reaction of *N-phenyl* or *N-meta*-chlorophenyl hydrazones (**b** and **c**, respectively) under analogous reaction conditions gave the cycloplatinated species **2b** and **2c** with the ligand as [C,N,N] terdentate. Treatment of the mononuclear complexes **1a** and **1d** with NaOAc (*n*-butanol, 100 °C) gave the corresponding cycloplatinated complexes **2a** and **2d**. Acetophenone hydrazone platinumacycle **2e** was prepared in a similar fashion and its reaction with tertiary mono and triphosphines gave mono or trinuclear species depending on the reaction conditions. The X-ray crystal structures of some of these complexes showed interesting π - π slipped stacking interactions between metallacyclic rings which, according to NCI analyses, showed aromatic character. Aimed to the rationalization of the different reactivity showed by acetylpyridine hydrazones and the precise role of acetate anion, the energy profiles for the three main steps for the cycloplatinated (iminoplatinum complex formation, chelation and cyclometallation) have been determined by DFT (M06) methods. Calculations indicate that cycloplatinated of **1b** proceeds *via* electrophilic substitution, involving the direct replacement of chloride anion at the Pt(II) centre by the *N-phenyl* moiety as the rate-determining step, to give an agostic intermediate **5b*** that, subsequently, undergoes elimination of a proton as hydrogen chloride. When present as an "external" base, acetate enters the coordination sphere around the Pt(II) centre and facilitates hydrazone N-H deprotonation and electrophilic C-H activation through a dissociative route, leading to a Wheland-type σ -complex intermediate **9ac**.

Introduction

In preceding decades, the chemistry of cyclometallated transition metal complexes has attracted much attention, in part due to their promising applications.¹ The most well-studied examples are five-membered metallacycles containing palladium,² being platinum complexes less frequently reported in spite of their interesting properties as, for example, electroluminescent properties useful in the design of light emitting devices found in compounds bearing tridentate ligands.³ The use of platinum complexes as anti-cancer metallodrugs is also well known⁴ (e.g. the activity of cyclometallated species with ligands structurally related to hydrazones has been widely studied).⁵

In the past, we have been interested in palladium(II) and

platinum(II) cyclometallated complexes bearing tridentate ligands⁶ and, particularly, cyclopalladated pyrimidin- and pyridazinhydrazones (examples **i**, **ii** in Chart 1) with *endo* geometry (i.e., with the carbon-nitrogen double bond inside the metallacycle) and acetylpyridine phenylhydrazones (**iii** in chart 1) with the *exo* coordination geometry. In these complexes the position of the C=N bond seemed to have no influence in the cyclometallation reaction, showing no evidence of the so-called "*endo effect*".⁷ We also studied the reactivity of complexes **i-iii** with different nucleophiles such as tertiary phosphines.^{8,9} Other palladium(II) examples with cyclometallated acetylpyridine phenylhydrazones acting as [C,N,N'] ligands¹⁰ or structurally related ligands¹¹ have also been reported. Examples with other metals¹² also appear in the literature but, to the best of our knowledge, no [C,N,N] Pt(II) analogues are yet known.

The crystal structures of **i-iii** and several of their derivatives showed interesting intermolecular between metallacyclic rings (i.e., rings involving at least one metal atom).⁸ Ghedini *et al.* reported one of the scarce examples showing such interactions in which the metallacycle is a cyclometallated ring;¹³ these interactions could also be a structural evidence¹⁴ of the so called "metalloaromaticity".¹⁵

^a Departamento de Química & Centro de Investigaciones Científicas Avanzadas (CICA), Universidade da Coruña. E-15008 La Coruña, Spain.

^b Departamento de Química Inorgánica, Universidad de Santiago de Compostela. E-15782 Santiago de Compostela, Spain.

† Electronic Supplementary Information (ESI) available: Synthetic and characterization details, Cartesian coordinates for all the computed molecules in XYZ format, Additional DFT computational results, Additional crystallographic data including inter- and intramolecular stacking parameters; CCDC 1536508 and 1536509. See DOI: 10.1039/C7DT03418K

ARTICLE

Journal Name

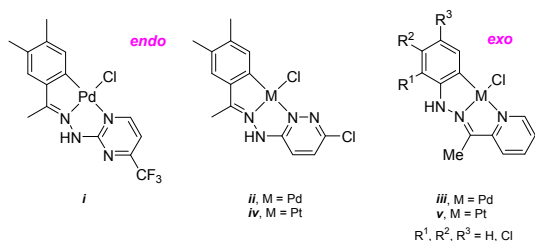


Chart 1

These type of interactions are attracting growing interest.^{16,17} For example, inter or intramolecular, interactions^{18,19} are known to modulate the luminescent behaviour of cyclometallated complexes and π stacking interactions are also paramount to explain the action mechanism of metallo-intercalators,²⁰ one type of antineoplastic drugs.

Thus, in view of the foreseeable applications of cyclometallated complexes with tridentate hydrazones and the lack of examples with platinum as central atom we sought to study the synthesis and reactivity of platinum(II) hydrazone cyclometallated complexes with the *endo* (*iv*) and *exo* (*v*) disposition of the imino group. The occurrence of inter- or intramolecular interactions in such complexes was also among the aims being pursued.

Consequently, herein we report the reaction of acetophenone and acetylpyridine hydrazones with $[PtCl_4]^{2-}$, to yield Pt(II) cyclometallated complexes with the ligand bonded in a tridentate [C,N,N'] fashion. Furthermore, since small structural differences, among other influential factors, seemed to convey rather large changes in the reactivity of the C–H activation patterns, we felt that the corresponding mechanism involved in the process should deserve a more detailed consideration, whereby we decided to study the feasible reaction pathways with the help of DFT calculations, which should also allow control of the factors governing the reactivity.

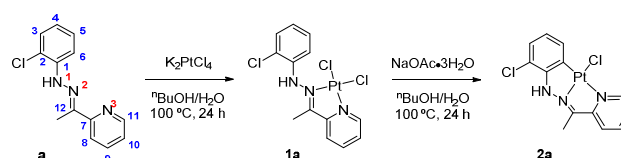
In addition, the reactivity of the acetophenone derivatives *iv* was also studied and complexes with the $(Ph_2PCH_2CH_2)_2PPh$ (triphos) ligand acting as [P,P,P] tridentate or the less common μ_3 bridging mode¹⁹ are described inclusive of X-ray crystal structure analysis for the latter case.

Where appropriate, the existence of intermolecular and intramolecular π – π stacking interactions involving metal chelate rings is discussed.

Results and discussion

Preparation of the cyclometallated complexes.

For the convenience of the reader the compounds and reactions are shown in Schemes 1–5. The compounds described in this paper were characterized by elemental analysis (C, H, N), by IR spectroscopy, and by 1H , ^{31}P - $\{^1H\}$ and ^{13}C - $\{^1H\}$ NMR spectroscopy, mass spectrometry and X-ray single crystal diffraction (data in the Experimental Section). All the spectroscopic and analytical data were in agreement with the proposed formulations (see Supplementary Information (SI) for an extended discussion).



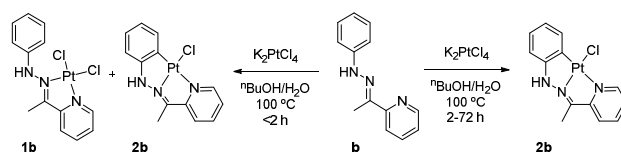
Scheme 1

endo-Platinacycles. Reaction of *N*-(2-chlorophenyl) hydrazone **a**, with $K_2[PtCl_4]$ in *n*-butanol/water at 100°C gave the non-cyclometallated complex $[Pt\{2-Cl-C_6H_4N(H)N=CMe(C_5H_4N)\}(Cl)_2]$ **1a** (See Scheme 1). Other reaction conditions ($K_2[PtCl_4]$ in ethanol/water at 60°C and $[Pt(\eta^3\text{-allyl})(\mu\text{-Cl})_2]$ in dry toluene at 60°C) also led to the [N,N'] coordination complex **1a**.

Following the pioneering discovery by Shaw *et al.* that the addition of NaOAc accelerated cyclometallation reactions,²¹ coordination complexes $[PtCl_2(k^2-N_{\text{imino}}, N_{\text{amino}})]$, which are analogous to **1a**, were converted into the corresponding terdentate [C,N,N'] cycloplatinated derivatives by reflux in a donor solvent in the presence of NaOAc.²² Therefore, we decided to test whether it was possible to obtain a cyclometallated derivative from the coordination complex **1a**. To our satisfaction, the synthesis of the desired cyclometallated monomer $[Pt\{2-Cl-C_6H_3N(H)N=CMe(C_5H_4N)\}(Cl)]$ **2a**, was accomplished by treatment of **1a** with a stoichiometric amount of NaOAc in *n*-butanol at 100°C. Thus, the effect of NaOAc on the C–H activation mechanism might be thermodynamic, by neutralizing the HCl formed during the reaction, kinetic by lowering the **1a/2a** activation barrier or by concurrence of both. In any case, no oxidative addition reaction of the C–Cl bond to give a Pt(IV) complex, as has been reported for similar complexes,²³ was observed.

Contrastingly, reaction of the *N*-phenyl hydrazone **b** with $K_2[PtCl_4]$ in *n*-butanol/water at 100°C for over 2 hours gave $[Pt\{C_6H_4N(H)N=CMe(C_5H_4N)\}(Cl)]$ **2b** (see Scheme 2). Reaction times under 2 hours gave a mixture of **2b** and $[Pt\{C_6H_5N(H)N=CMe(C_5H_4N)\}(Cl)_2]$ **1b**, from which the latter could not be isolated. NaOAc was added to the mixture of **1b** and **2b** in *n*-butanol with the intention of shift the reaction toward **2b** but heating of this solution led to the immediate formation of black platinum.

The signals corresponding to **1b** could be identified in the 1H NMR spectrum of the reaction mixture and showed similar characteristics to those described for the analogue, **1a** (see Experimental Section and SI). Incidentally, compound **2b** could also be prepared by reaction of **b** with $[Pt(\eta^3\text{-allyl})(\mu\text{-Cl})_2]$ in dry toluene at 60 °C.

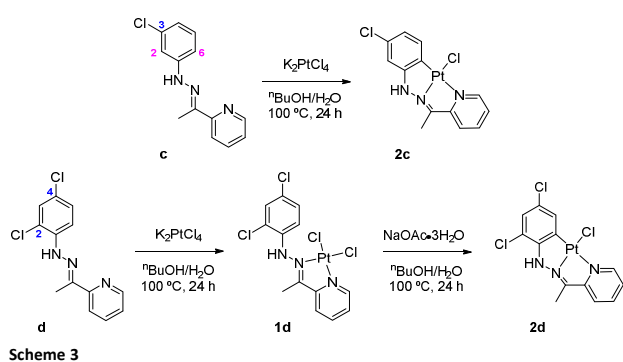


Scheme 2

These results seem to indicate that the non-cyclometallated complexes **1a** and **1b** are formed in first place. However, whilst C-H activation of **1b** happens spontaneously with longer reaction times, the **1a/2a** activation barrier seems to be higher and NaOAc is needed to lower this barrier.

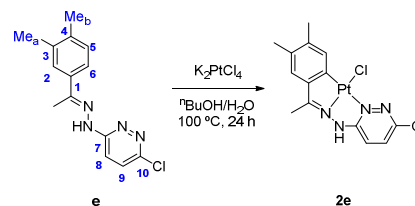
The different behaviour led us to study the detailed mechanism and role of acetate in the process by DFT methods (*vide infra*). The understanding gained with the computational model prompted us to further explore the same reaction process with other ligands characterized by the presence of a 3-chlorophenyl (ligand **c**) or a 2,4-dichlorophenyl substituent (ligand **d**) at the amino group (see Scheme 3). Under similar reaction conditions, reaction of **c** with $K_2[PtCl_4]$ in *n*-butanol/water at 100°C for 24 hours afforded the cyclometallated complex $[Pt\{3-Cl-C_6H_3N(H)N=CMe(C_5H_4N)\}(Cl)]$, **2c**. Thus, metallation of **c** was direct and regioselective at position 6, in the less hindered site and in *para* relationship with the chlorine substituent. Conversely, reaction of **d** with $K_2[PtCl_4]$ in *n*-butanol/water at 100°C gave $[Pt\{2,4-Cl-C_6H_3N(H)N=CMe(C_5H_4N)\}(Cl_2)]$, **1d** which, upon treatment with a stoichiometric amount of NaOAc in *n*-butanol/water at 100°C for 24h, gave the corresponding cyclometallated complex $[Pt\{2,4-Cl-C_6H_2N(H)N=CMe(C_5H_4N)\}(Cl)]$, **2d**, in a similar manner to **2a**. Complexes **2c**, **1d** and **2d** showed similar spectroscopic characteristics to those described for the **a** and **b** derivatives (see Experimental Section and SI).

Therefore, ligands could be grouped in two categories according to their behaviour toward C-H activation by $K_2[PtCl_4]$. **b** and **c** yielded directly the metallated species **2b** and **2c**, but **a** and **d** did not produce C-H activation under similar conditions, and treatment of the resulting coordination compounds **1a** and **1d** with NaOAc was necessary in order to metallate the ligands. This seems to indicate that C-H activation in *meta* to one or two electron-withdrawing chlorine substituents may not be accomplished by treatment with $K_2[PtCl_4]$ in *n*-butanol/water. However, C-H activation could be promoted by NaOAc, in the second reaction stage.



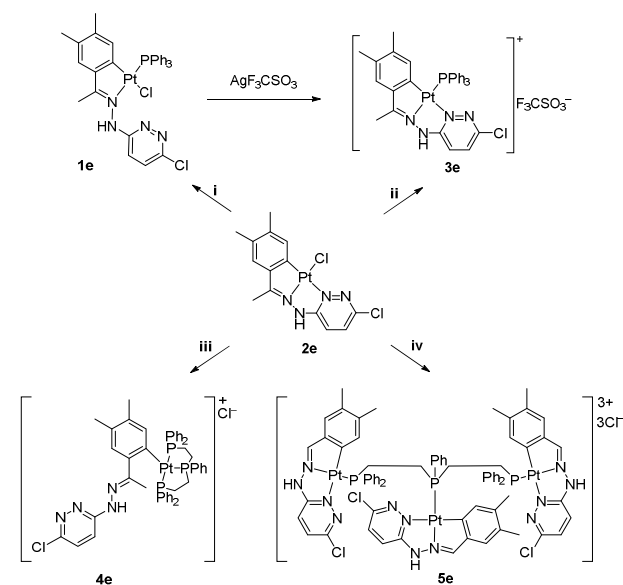
exo-Platinacycles. In order to synthesize Pt(II) complexes containing a tridentate [C,N,N'] hydrazone ligand but showing an *exo* geometry, we decide to study the reactivity of ligand **e** with $K_2[PtCl_4]$. Regardless the reaction conditions

[ethanol/water at 60°C or *n*-butanol/water at 100°C for 24h] the cyclometallated complex $[Pt\{3,4-Me_2-C_6H_2C(Me)=NN(H)(4'-Cl-C_4H_2N_2)\}(Cl)]$ **2e** with the imine group in the *endo* position was obtained (see Scheme 4). Non-cyclometallated complexes analogous to **1a** and **1b** were not observed.



The low solubility of **2e** precluded its characterizations in solution, however, the structure of the derivatives **1e** and **3e-5e**, *vide infra*, was in agreement with the structure proposed. Moreover, recrystallization of **2e** from dimethyl sulfoxide gave crystals of the new complex **2e-dmso** with the chloride ligand replaced by a dimethyl sulfoxide molecule and deprotonation of the hydrazinic nitrogen atom.

Reaction of **2e** with triphenylphosphine, gave $[Pt\{(3,4-Me_2-C_6H_2C(Me)=NN(H)(4'-Cl-C_4H_2N_2)\}(Cl)(PPh_3)]$, **1e**, in which the phosphine is coordinated to the metal atom after ring opening (see Scheme 5, Experimental Section and SI for characterization details). Ring opening could be avoided by treatment of **2e** with silver trifluoromethanesulfonate, prior to reaction with the phosphine. Under these reaction conditions $[Pt\{(3,4-Me_2-C_6H_2C(Me)=NN(H)(4'-Cl-C_4H_2N_2)\}(PPh_3)][F_3CSO_3]$, **3e**, was obtained. Compound **3e** was also prepared by reaction of **1e** with silver trifluoromethanesulfonate in acetone.



Scheme 5. i) PPh_3 (acetone, 1:1 molar ratio), ii) 1: AgF_3CSO_3 , 2: PPh_3 (acetone, 1:1 molar ratio), iii) triphos (acetone, 1:1 molar ratio), iv) triphos (acetone, 3:1 molar ratio).

ARTICLE

Journal Name

Reaction of **2e** with the tertiary triphosphine (Ph₂PCH₂CH₂)₂PPh (triphos), in a 1:1 molar ratio, gave [Pt{(3,4-Me₂-C₆H₂C(Me)=NN(H)(4'-Cl-C₆H₄N₂))(Ph₂PCH₂CH₂)₂PPh-P,P,P][Cl], **4e**, as air-stable 1:1 electrolyte, which was fully characterized. Treatment of **2e** with (Ph₂PCH₂CH₂)₂PPh, in a 3:1 molar ratio, gave a green solid, sparingly soluble in most of the common solvents (see Experimental Section and SI for characterization details). Fortunately, a small number of crystals of **5e** suitable for X-ray diffraction were grown from a chloroform solution of this complex (*vide infra*)

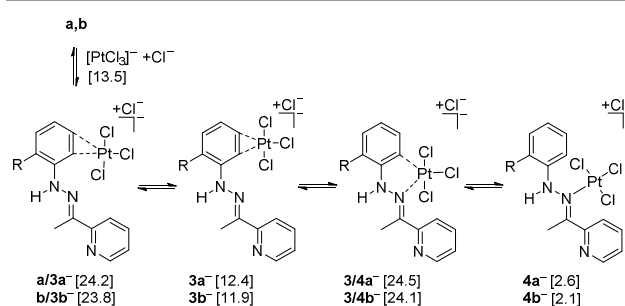
Computational study of the cyclometallation of acetylpyridine hydrazones promoted by [PtCl₄]²⁻

Due to its industrial relevance and synthetic applications, mechanistic aspects of C-H activation by metal complexes have inspired a number of experimental and theoretical investigations,²⁴ including studies on methane activation reactions mediated by [PtCl₂(H₂O)₂], [PtCl₂(NH₃)₂], [Pt(bpym)Cl₂] (bpym = 2,2'-bipyrimidine) or [Pt(HPzm)₂Cl₄] (HPzm = pyrazolium) complexes (Shilov system)²⁵ and arene C-H activation²⁶ or roll-over cyclometallations²⁷ promoted by Pt(II) complexes with chelating ligands bearing nitrogen donor atoms. Nevertheless, computational studies on the cycloplatination reaction mechanism are scarce, and are mainly related to electron-rich platinum(II) complexes which cyclometallate with liberation of methane. For these processes, multistep mechanisms have been proposed, involving ligand dissociation to a coordinatively unsaturated intermediate which subsequently undergoes an intramolecular oxidative-addition/reductive elimination sequence.²⁸ In this manner, although [PtCl₄]²⁻ and [PtCl₂(solv)] are common metal precursors in cycloplatination reactions,^{5a,29} the energy profile for arene cyclometallation reactions promoted by [PtCl₄]²⁻ has not been previously computed.³⁰ In an effort to gain useful insight and understanding of the factors accounting for the differential behavior of acetylpyridine hydrazones **a-d** in cyclometallations promoted by [PtCl₄]²⁻, we sought out to study the possible reaction pathways by using M06 DFT methods in conjunction with the polarizable continuum solvation model (see Computational Methods in the SI).

Cycloplatination of ligand b. Firstly, we carried out a study on the reaction between ligand **b** and [PtCl₄]²⁻ in the aforementioned conditions, considering associative, dissociative and concerted (interchange) mechanisms for the chloride substitution on Pt(II) centre, with either pyrido, imino, amino or benzene moieties acting as nucleophiles. For the C-H bond cleavage event we considered the electrophilic substitution (via Wheland-type intermediate), the σ-bond metathesis and the oxidative addition pathways. For a complete representation of all the mechanistic possibilities that have been computed see Schemes S3A,B in the SI.

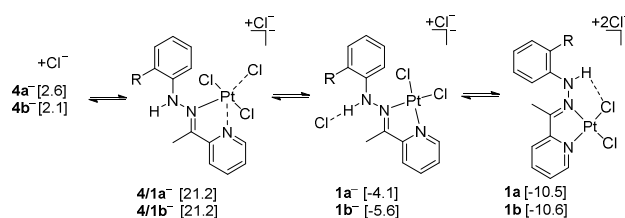
According to DFT calculations, reaction initiates with dissociation of [PtCl₄]²⁻ to yield chloride anion and [PtCl₃]⁻, in a solvent assisted process, through a Pt(II) square-planar intermediate. Such dissociation was unfavorable by 13.5 kcal/mol, and required an activation energy of 30.1 kcal/mol

(see SI, Scheme S4).³¹ Next, the reaction of [PtCl₃]⁻ with ligand **b** takes place by coordination to the phenyl group (see Scheme 6). Going through transition structure **b/3b⁻**, such coordination requires an activation energy of 10.3 kcal/mol and gives rise to a η²-(C,C)-bonded³² intermediate complex **3b⁻** which lies 11.9 kcal/mol higher in energy than the separate starting compounds (**b** and [PtCl₄]²⁻, selected as reference for the energy profile) but results 1.6 kcal/mol lower in energy than **b**, chloride anion and [PtCl₃]⁻ (see Figures 1 and 3). Subsequently, intermediate **3b⁻** rearranges to the mono-coordinated iminoplatinum(II) derivative **4b⁻**,^{33,34,35} which was found 2.1 kcal/mol above the starting reagents. Going through transition structure **3/4b⁻**, this rearrangement can proceed in one step with an activation energy of 12.2 kcal/mol. Competitive pathways to intermediate **4b⁻**, involving other dissociative routes, nucleophilic substitutions at [PtCl₄]²⁻ or solvated [PtCl₃]⁻ (via five-coordinate transition states)³⁶ or direct activation of the C-H bond were found higher in energy (see SI, Schemes S5-S8).



Scheme 6. Reaction of ligand **a,b** with [PtCl₄]²⁻ to form iminoplatinum complex **4a,b⁻**. Relative free energies (kcal/mol) calculated in butanol solution at 373 K are shown in brackets.

From mono-coordinate intermediate **4b⁻** two possible reaction pathways have been computed: the first one, the cyclometallation at the phenyl ring, involves a considerably energy penalty (30.7 kcal/mol or higher, see SI, Scheme S9). Instead, chloride substitution at Pt(II) by the pyridine nitrogen, via the five-coordinate transition structure **4/1b⁻**, showed a lower activation energy (19.1 kcal/mol, see Scheme 7) and led to chelate complex **1b**, with the acetylpyridine hydrazone acting as [N,N] bidentate ligand.

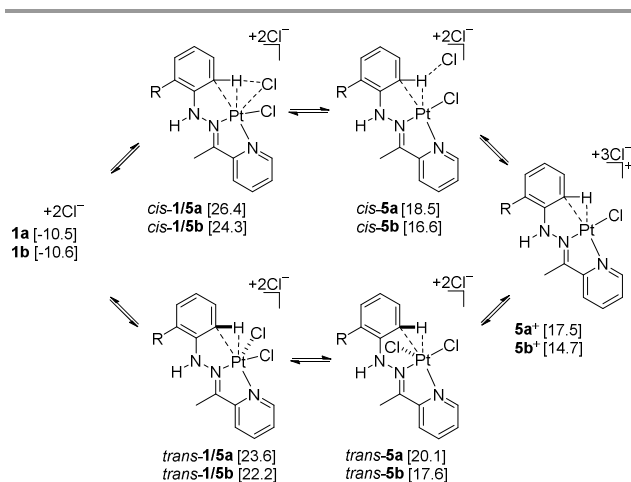


Scheme 7. Formation of intermediate **1a,b** by chelation of iminoplatinum complex **4a,b⁻**. Relative free energies (kcal/mol) calculated in butanol solution at 373 K are shown in brackets.

Chelate intermediate **1b** was characterized by an intramolecular hydrogen bond between the hydrazone

hydrogen and a chloride ligand, and was calculated as the most stable species in the reaction pathway, lying 10.6 kcal/mol below the starting compounds.³⁷ Thus, according to DFT calculations, cycloplatination of ligand **b** with $[\text{PtCl}_4]^{2-}$ takes place by initial iminoplatinum complex formation followed by chelation. These two steps were calculated as exergonic and did not determine the rate of the cycloplatination process (*vide infra*).

Lowest energy pathway for the cyclometallation of chelate complex **1b** followed an electrophilic substitution process involving the cationic intermediate **5b⁺**, which was calculated 14.7 kcal/mol above starting compounds (see Scheme 8).



Scheme 8. Formation of agostic intermediate **5a,b⁺** from the chelate **1a,b**, by direct replacement of the chloride anion at Pt(II) by the *N*-phenyl moiety. Relative free energies (kcal/mol) calculated in butanol solution at 373 K are shown in brackets.

The associative route provided the most favoured transition structures for the electrophilic activation, by direct nucleophilic displacement of a chloride ligand from the Pt(II) centre by the *N*-phenyl group. Such transition structures, *cis*-**1/5b** and *trans*-**1/5b**, and the resulting ion-pair intermediates *cis*-**5b** and *trans*-**5b**, were characterized by either a *cis* or a *trans* relationship between the activated C-H bond and the leaving chloride. The ion-pairs (*cis*-**5b** and *trans*-**5b**) and the cationic intermediate (**5b⁺**) exhibit a close proximity of the C-H bond to the metal, revealed by a short Pt-H contact (1.96–2.04 Å), an elongated C-H distance (1.13–1.17 Å) and a wide Pt-H-C angle (79.0–86.0°), which are indicative of an agostic interaction (see Figure 1).³⁸ Such agostic interaction seems to be incipient in the transition structures *cis*-**1/5b** and *trans*-**1/5b** and may contribute to reduce the energy barrier for the cycloplatination.³⁹ Moreover, in transition structure *cis*-**1/5b** the agostic interaction is sufficient to polarize the C-H bond and allow the leaving chlorine atom to establish an intramolecular hydrogen-bond like contact that becomes fully developed at the resulting ion-pair intermediate *cis*-**5b**. Nevertheless, calculations indicate that transition structure *trans*-**1/5b**, which required an activation energy of 32.8 kcal/mol from the chelate intermediate,⁴⁰ was favoured over *cis*-**1/5b** by 2.1 kcal/mol. Similar associative transition states

have been implicated in other theoretical works on C-H activation catalyzed by Pt(II) complexes with chelating N-based ligands,⁴¹ but this is, to the best of our knowledge, the first time a *trans* relationship between the incoming C-H bond and the ligand being displaced from the metal centre is reported. Other alternative cyclometallation pathways have also been taken into account but required higher energy barriers (see SI, Schemes S10–S15).

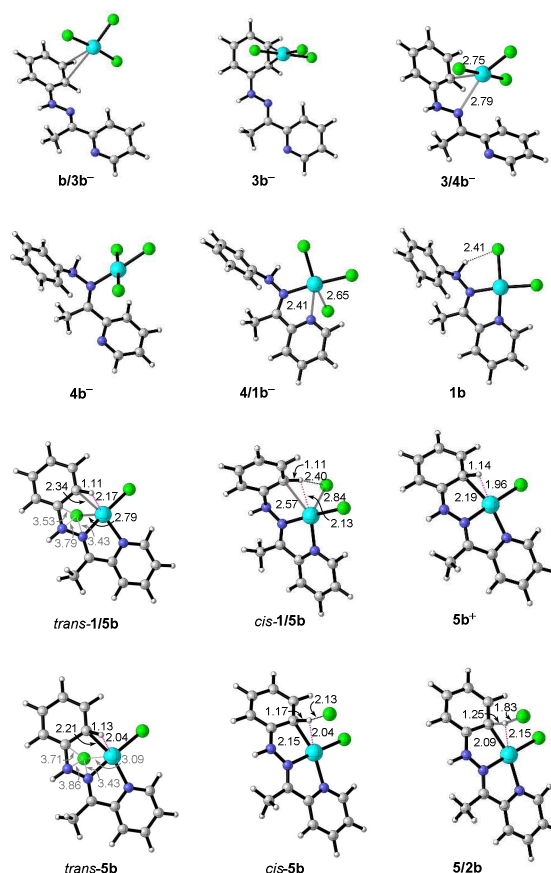


Figure 1. Optimized geometries of intermediates and transition structures in the lowest energy route to **2b**. Bond lengths and interaction distances are in Angstroms.

The preference for transition structure *trans*-**1/5b** over the *cis*-**1/5b** counterpart may be originated by an incipient non-covalent interaction between the leaving chloride ligand and the π -system of the *N*-phenyl hydrazone moiety, which is becoming acidic in the associative transition structures. Accordingly, in *trans*-**1/5b** the distances between the leaving chloride and N1, N2, N3, C1, C5, C7 and C12 of the *N*-phenyl hydrazone moiety (3.43–4.47 Å) are significantly shorter than the corresponding values in *cis*-**1/5b** (3.56–4.73 Å, see SI, Table S2). Description of the charge-transfer interactions in transition structures *cis*-**1/5b** and *trans*-**1/5b** was obtained by

ARTICLE

the second-order perturbation theory analyses of Fock matrix in the natural bond orbital (NBO) basis⁴² (see SI, Table S2).

To obtain further insight into these non-covalent interactions (NCI) the NCI index was computed for *trans*-**1/5b**.⁴³ Simple visual inspection of the NCI isosurfaces calculated for *trans*-**1/5b** (see Figure 2) reveals red cigars for repulsive steric clashes inside the rings, a deep blue almond-shaped surface for the incipient stabilizing agostic interaction with a small red line inside (due to steric strain of the forming 3-membered ring), a light blue pill-like surface for the breaking Pt-Cl bond (weaker than regular stabilizing interaction) and green flat isosurfaces for the van der Waals interactions. In particular, a light blue region in the greenish extended form is clearly identified next to the leaving chloride atom, revealing an attractive dispersion interaction with the C1 atom at the *N*-phenyl moiety (corresponding to an attractive peak at $\rho = -0.006$ a.u. in the $s(\rho)$ diagram, see SI, Figure S1).

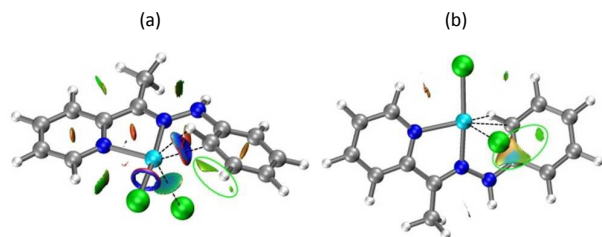
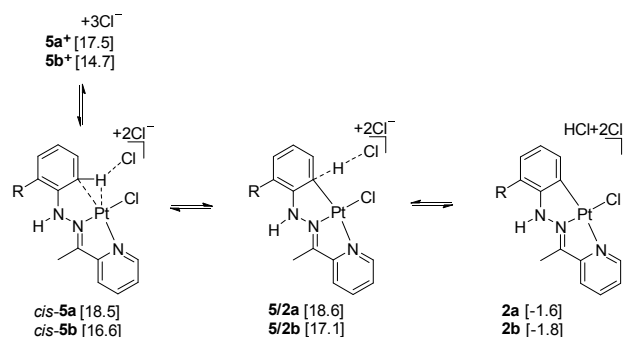


Figure 2. NCI analysis of transition structure *trans*-**1/5b**. Gradient isosurfaces are colored on a BGR scale, according to the values of $\text{sign}(\lambda_2)\rho$: blue for attractive interaction, green for weak interaction and red for repulsive steric clashes. Region of weakly non-bonding interactions between leaving chloride and *N*-phenylhydrazone moiety highlighted in green. (a) NCI isosurface with $s = 0.3$, color scale in the $-0.07 < \text{sign}(\lambda_2)\rho < 0.05$ au range. (b) NCI isosurface with $s = 0.5$ with a density cut-off of $\rho = 0.008$, color scale in the shorter $-0.011 < \text{sign}(\lambda_2)\rho < 0.011$ au range, to highlight the differences between attractive and repulsive dispersion interactions.

Finally, a chloride anion acts as a base and intermediate **5b⁺** loses the C-H hydrogen and yields the cyclometallated product **2b** and hydrogen chloride (see Scheme 9). Although the association of chloride to the activated C-H bond in **5b⁺** to form the intermediate ion-pair complex *cis*-**5b** was endergonic in 1.9 kcal/mol, most stable transition structure for the elimination step (**5/2b**) was located only 2.4 kcal/mol above the cationic precursor **5b⁺**.

Calculations indicate that cyclometallated complex **2b** is 8.8 kcal/mol higher in energy than the coordination intermediate **1b**, assuming that all the reaction products are isolated within the solvent reaction field and hydrogen chloride is not ionized (see Schemes 8 and 9). Thus, considering the microscopic reversibility of the process, protonolysis of the C-Pt bond in **2b** would be significantly more rapid than the C-H activation step. Therefore, the formation of the cyclometallated complex with good yield could be only explained if the hydrogen chloride formed as side-product is ionized and partially neutralized by the solvent mixture.^{44,45}



Scheme 9. Elimination of HCl from agostic intermediate **5a,b⁺** to give the cyclometallated complex **2a,b**. Relative free energies (kcal/mol) calculated in butanol solution at 373 K are shown in brackets.

Cycloplatination of ligands a, c and d. With comparative purposes, the cyclometallation of ligand **a**, with the chlorine substituent at the phenyl ring, has also been computed (see Schemes 6-9). In solution, lowest energy route to cyclometallated complex **2a** also involved initial formation of an iminoplatinum complex **4a**, subsequent chelation to **1a** and then cycloplatination by an electrophilic substitution, with direct displacement of a chloride atom at the Pt(II) centre, going through *trans*-**1/5a** in the rate-determining step to the agostic ion-pair intermediate *trans*-**5a**. Even though the energy profiles in solution are similar for series **a** and **b** (see Figure 3), some quantitative differences were found. Firstly, the activation energies for electrophilic attack of $[\text{PtCl}_3]^-$ to ligands **a** and **b** (going through transition structures **a/3a⁻** and **b/3b⁻**) are 24.2 and 23.8 kcal/mol, respectively. Secondly, the relative energies computed for chelate intermediates **1a** and **1b** are very similar, but transition structure *trans*-**1/5a** and intermediate *trans*-**5a** are calculated higher in energy than *trans*-**1/5b** and *trans*-**5b** by 1.4 and 2.5 kcal/mol, respectively. Thus, it seems that the presence of the electron-withdrawing chlorine substituent reduces the nucleophilic character of the *N*-phenyl group in the ligand and the chelate intermediate and also destabilizes the agostic intermediate.⁴⁶ Thirdly, the presence of the chlorine also reduces the speed of the final elimination step. In this manner, the activation energy for deprotonation of intermediate *cis*-**5a** (leading to transition structure **5/2a**) was calculated 1.5 kcal/mol higher than that required to reach transition structure **5/2b**.

Considering that ligands **c** and **d** may probably follow in their cycloplatination processes the same route as ligands **a** and **b**, we have also located the most favoured structures for the chelated intermediates **1c** and **1d**, the agostic intermediates **5c⁺** and **5d⁺** and the transition structures connecting them through a direct electrophilic substitution process. As previously found for the series **a** and **b**, transition structures *trans*-**1/5c** and *trans*-**1/5d**, with a *trans* relationship between the leaving chloride and the incoming C-H bond, were calculated lower in energy than the *cis* counterparts (see SI, Schemes S16A,B). In agreement with the experimental trend, the activation energies calculated for the cyclometallation of ligands **b** and **c** by direct electrophilic substitution (going

through *trans*-**1/5b** and *trans*-**1/5c**, respectively) resulted very similar (33.0±0.2 kcal/mol) and lower than those calculated for the corresponding cyclometallations of ligands **a** and **d** (34.1 and 35.8 kcal/mol, respectively) which were not experimentally observed in 1-butanol at 373 K.

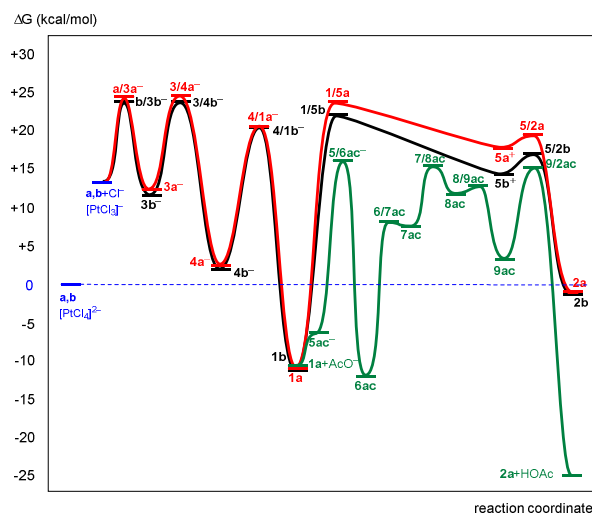


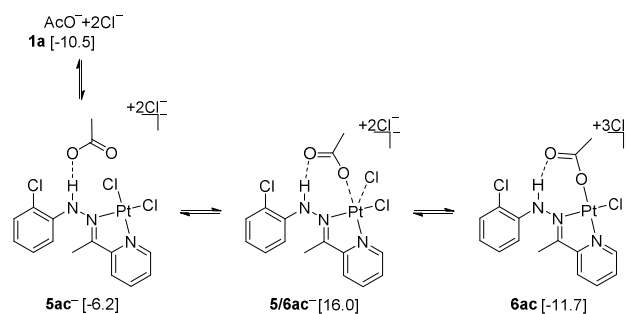
Figure 3. Schematic energy profiles for the reaction of acetylpyridine hydrazones **a,b** with $[\text{PtCl}_4]^{2-}$ in butanol at 373K.

Cycloplatination of 1a in the presence of acetate anion. Next we explored the possible reaction pathways for the cycloplatination of chelate intermediate **1a** in the presence of acetate anion (denoted as series **ac** in the Schemes 10-12 and Figures 3 and 4).

Acetate anion has been used as an external base to assist cyclometallations on coordination complexes $[\text{PtCl}_2(\kappa^2\text{-}N_{\text{imino}}, N_{\text{amino}})]$ which are analogous to **1a**.²² In particular, for the cycloplatination of aryl imines promoted by $[\text{cis-Pt}(\text{dmsO})_2\text{Cl}_2]$ and NaOAc in MeOH, kinetic studies at variable temperature and pressure indicated the formation of an acetate-substituted intermediate complex $[\text{PtCl}(\text{OAc})(\kappa^2\text{-}N_{\text{imino}}, N_{\text{amino}})]$, that could be only detected by NMR spectroscopy.^{22c} The kinetic and activation parameters were interpreted in terms of a C-H activation event *via* electrophilic substitution, through a highly ordered and compressed transition state, involving the C-H and the Pt-O(acetate) bonds. Such four-centered transition state should be very similar to that proposed for equivalent cyclopalladations.⁴⁷ Cycloplatinations of N,N',N'' -triarylguanidines with *cis*- $[\text{Pt}(\text{dmsO})_2\text{Cl}_2]$ and NaOAc in MeOH have also been reported to produce intermediate acetate complexes $[\text{PtCl}(\text{dmsO})(\text{OAc})(\kappa^1\text{-}N_{\text{imine}})]$, that could be isolated and crystallographically characterized.^{35b} From these acetate-bound Pt(II) complexes, by analogy with cyclopalladations on related systems,^{24c,48} the metallation event was presumed to follow either an ambiphilic metal-ligand activation (AMLA) or a solvent-assisted concerted metalation-deprotonation (CMD) pathway, involving six-membered transition states. The mechanistic proposals for these cycloplatinations were not supported by computational methods. In fact, until now, only two theoretical investigations have been devoted to the

carboxylate-assisted C-H activations at platinum centres.⁴⁹ Sasaki *et al.* reported the key features in the C-H bond activation of benzene by $[\text{Pt}(\kappa^2\text{-O}_2\text{CH}_2)_2]$.⁵⁰ The process involves initial $\kappa^2\text{-}\kappa^1$ displacement of formate ligand to give a σ -complex intermediate, followed by heterolytic cleavage of the C-H bond through a six-membered transition structure, where the dangling oxygen of the monodentate acetate ligand abstracts the proton (AMLA-6). A similar two-step mechanism was reported by Goddard, Periana *et al.* for benzene activation at $[\text{Pt}(\text{bpym})\text{TFA}_2]$ and $[\text{Pt}(\text{pic})\text{TFA}_2]^-$ (pic = $\kappa^2\text{-}N,O$ -picolinate),^{26b} where the trifluoroacetate ligand facilitated the activation event.⁵¹

Thus, for the computational study of the cycloplatination of chelated intermediate **1a** in the presence of NaOAc, in addition to electrophilic substitution and oxidative addition pathways, we also considered concerted metallation and proton abstraction (ambiphilic activation) to acetate, which could either coordinate previously to the Pt(II) centre displacing chloride (intramolecular assisted path) or not (intermolecular assisted path). Computations indicate that cyclometallation of chelate **1a** in the presence of acetate anion initiates with a hydrogen bond interaction between acetate and the hydrazone hydrogen leading to complex **5ac**, which lies 4.3 kcal/mol above the separate precursors (see Scheme 10). Next, intermediate **5ac** undergoes internal displacement of chloride by acetate at the Pt(II) centre, to afford the complex **6ac** in an exergonic process.³⁶ The energy penalty for this ligand exchange via transition structure **5/6ac** was 22.2 kcal/mol, and the chelate intermediate **6ac** was favoured by 1.2 kcal/mol over the separate precursors, acetate and chelate **1a**. Formation of intermediate **6ac** by direct displacement of chloride by acetate on chelate **1a** was calculated higher in energy (see SI, Scheme S17). In this manner, computational results are consistent with previous experimental findings for related cyclometallations with platinum group precursors: when present in the reaction medium, acetate enters the coordination sphere around the Pt(II) centre in the chelated intermediate **1a** and gives rise to an intermediate acetate complex **6ac**.



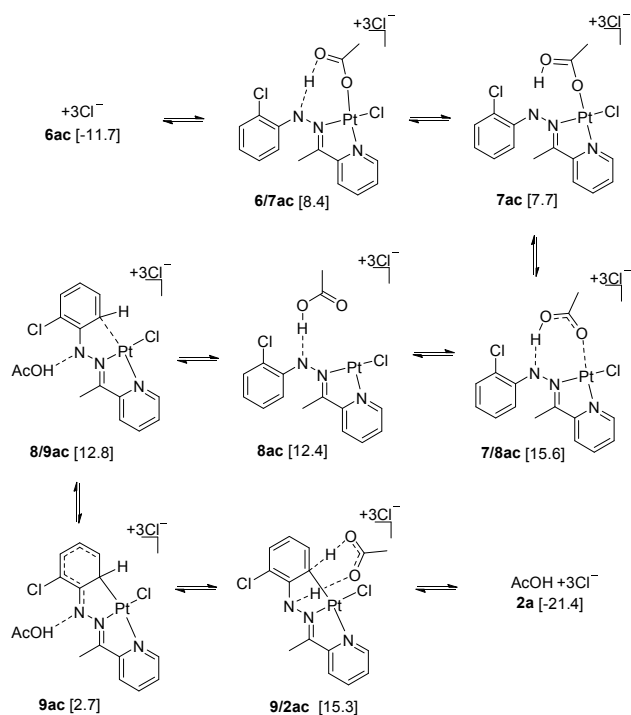
Scheme 10. Entrance of acetate in the coordination sphere of Pt(II). Relative free energies (kcal/mol) calculated in butanol solution at 373 K are shown in brackets.

Once coordinated to the Pt(II) centre, acetate acts as an internal proton-abstracting base and facilitates the cyclometallation by an electrophilic substitution involving the

ARTICLE

Journal Name

neutral Wheland-type σ -complex intermediate **9ac**, which lies only 2.7 kcal/mol above starting compounds plus acetate (see Scheme 11).⁵²



Scheme 11. Cyclometallation of the acetate bound chelate intermediate **6ac** through the coordinatively unsaturated complex **8ac** and the Wheland intermediate **9ac**. Relative free energies (kcal/mol) calculated in butanol solution at 373 K are shown in brackets.

Calculations indicate that the dissociative pathway, leading to the 14-electron, T-shaped intermediate **8ac** is favoured over the associative ones by more than 5.3 kcal/mol (see SI, Schemes S18A,B).⁵³ In this manner, from the acetate bound Pt(II) complex **6ac**, an intramolecular proton transfer from the hydrazone to the carbonyl oxygen, going through the six-membered transition structure **6/7ac**, requires an activation energy of 20.1 kcal/mol and affords the acetic acid bound intermediate **7ac**. Next, the lowest energy channel to zwitterionic intermediate **8ac** involves the seven-membered transition structure **7/8ac**, with an activation energy of only 7.9 kcal/mol, where the acetic acid ligand dissociates from the Pt(II) centre but maintains a hydrogen bond interaction with the hydrazone nitrogen. An intramolecular proton transfer from an N-H group to acetate has been previously characterized by DFT methods for Pd(OAc)₂ catalyzed C-H bond functionalization⁵⁴ but has no precedents in the platinum group metal-mediated cyclometallations. It appears that the proton transfer increases the leaving group ability of the acetate ligand as well as the electron-donating character of the bidentate hydrazone ligand, and thus, opens a dissociative pathway of lower activation energy for the electrophilic activation for the resulting acetic acid/hydrazone bound Pt(II) complex. ^{7c,55} It can be concluded that the presence of an acidic N-H bond in the neighbourhood of the acetate bound

Pt(II) centre may account for the inversion of the prevalent reaction sequence, so that the acetate-mediated deprotonation (of the N-H bond) and departure of the acetic acid ligand takes place previously to the C-H activation event.

The zwitterionic intermediate **8ac** shows the carbonyl group of the acetic acid moiety pointing to the metal, with the carbonyl oxygen placed 3.51 Å away from the Pt(II) centre (see Figure 4), which may be indicative of a non-covalent interaction.⁵⁶ The hydrogen bond interaction between the acetic acid and the hydrazone nitrogen, which places the acetic acid moiety in the second coordination sphere of the Pt(II) centre, was also present in the subsequent associative transition structure **8/9ac** and the resulting σ -complex intermediate **9ac**, with O-H...N distances close to 1.8 Å (see Figure 4). Most stable transition structure **8/9ac** for the nucleophilic attack of the phenyl group to the coordinatively unsaturated Pt(II) centre was located early in the bond making process, only 0.4 kcal/mol above precursor **8ac**.

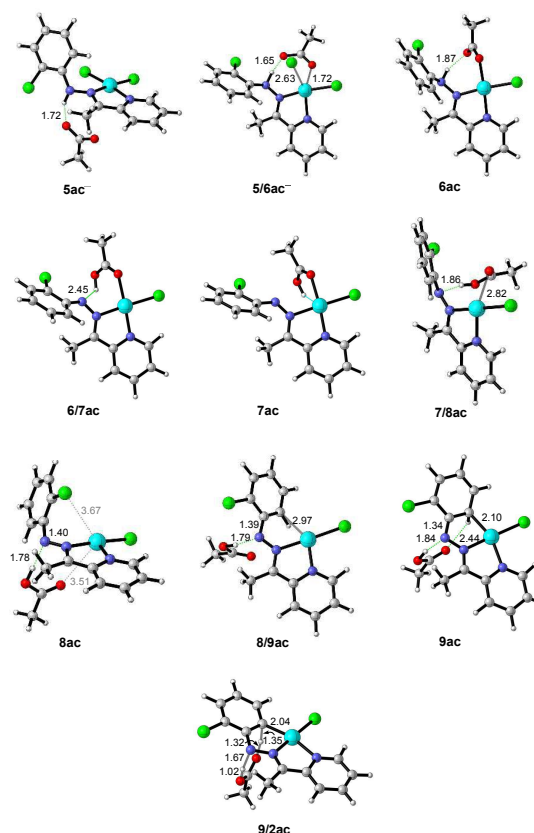


Figure 4. Optimized geometries of intermediates and transition structures for the cycloplatination of chelate **1a** in the presence of acetate anion. Bond lengths and interaction distances are in Angstroms

Transition structure **8/9ac** showed a wide C-Pt bond forming distance (2.97 Å, without any incipient Pt-H contact) and a *cis* relationship between the hydrogen-bound acetic acid moiety and the activated C-H bond. Alternative cyclometallation pathways involving other dissociative routes for electrophilic

substitution or oxidative C-H addition followed by reductive elimination have also been taken into account but required higher energy barriers (see SI, Schemes S19-S20). Despite repeated attempts, transition structures for the routes involving concerted metalation and proton abstraction to acetate (CMD) were not located.

Wheland-type σ -complex⁵⁷ intermediate **9ac** was assigned arenonium ion (cyclohexadienyl cation) character due to its shortened C-N(amine) bond length (1.34 Å), small but noticeable puckering of the phenyl moiety (C(1)C(2)C(3)C(4) dihedral angle of 10.9°), short Pt-C bond length and weak Pt-H contact (2.10 and 2.26 Å, respectively), probably consequence of the strong donating ability of the hydrazonate moiety.⁵⁸ Wheland-type intermediate **9ac** was also characterized by the close proximity of the C-H bond to the carbonyl oxygen of the acetic acid moiety, which may be indicative of a second hydrogen bond-like interaction (H...O distance of 2.44 Å and C-H...O angle of 135.0°). Hence, aromatization of Wheland-type σ -complex intermediate **9ac** and reprotonation of the hydrazonate nitrogen can take place in one step, going through the eight-membered transition structure **9/2ac**, with an energy penalty of only 12.6 kcal/mol. In transition structure **9/2ac** the hydrogen bound acetic acid molecule donates a proton to the hydrazonate nitrogen and simultaneously accepts the proton from the activated C-H bond. Finally, the cyclometallation of **1a** to **2a** in the presence of 1 equivalent of acetate as auxiliary base becomes exergonic in 10.9 kcal/mol. Accordingly with the computational results we can conclude the following:

(1) Cyclometallation of acetylpyridine *N*-phenylhydrazones **a,b** promoted $[\text{PtCl}_4]^{2-}$ take place in three consecutive processes, involving initial iminoplatinum complex formation, followed by chelation and then final cycloplatination. While formation of the intermediate chelate complexes **1a** and **1b** is thermodynamically favoured, cycloplatinations to **2a** and **2b** are calculated as endergonic processes. Hence, isolation of cyclometallated complex **2b** may be explained if the hydrogen chloride formed as side-product is ionized and partially neutralized by the solvent mixture.

(2) With difference to related cycloplatinations which take place with liberation of methane,²⁸ lowest energy pathway for the cyclometallation of chelate complex **1b** in butanol at 373 K involves an electrophilic substitution process. In this manner, initial nucleophilic displacement of chlorine from the Pt(II) centre by the phenyl group in the rate-determining step leads to an intermediate agostic complex that subsequently loses HCl in the final aromatization step. Most favoured associative transition structure located for the arene activation event showed an unprecedented *trans* relationship between the incoming C-H bond and the ligand being displaced from the metal centre.

(3) Isolation of the non-cyclometallated complexes **1a** (or **1d**) in the same reaction conditions can be understood as a consequence of an increased activation energy for the nucleophilic attack of the *N*-phenyl moiety to the Pt(II) centre, due to the presence of the electron withdrawing chlorine substituent(s), that may reduce the rate of cyclometallation in

a sufficient extension to enable accumulation and isolation of the intermediate.

(4) In the presence of NaOAc as an auxiliary base, the cyclometallation of **1a** to **2a** and acetic acid as side-product becomes a thermodynamically favoured process. When present in the reaction medium, acetate enters the coordination sphere around the Pt(II) centre in the rate-determining step and facilitates subsequent hydrazone N-H deprotonation and electrophilic C-H activation following a dissociative route of lower activation energy. Thus, initial dissociation of acetic acid ligand leading to a coordinatively unsaturated Pt(II) complex is followed by association of the phenyl group, formation of a Wheland-type σ -complex intermediate and final aromatization.

Crystal structures of **2e-dmso** and **5e**.

The molecular structures of **2e-dmso** and **5e** are illustrated in Figures 5 and 9, respectively. Crystal data, and selected bond distances and angles (Table S6) are given in the SI. Complete intramolecular π - π stacking parameters are also in the SI (Table S3).

The asymmetric unit of **2e-dmso** contains one-half molecule of the complex with all its non-hydrogen atoms, except the dmso methyl, lying in the (0 4 0) crystallographic mirror plane. In the molecule the platinum atom is bonded in a slightly distorted square-planar geometry to the C(1) carbon atom of the phenyl ring, the N(1) and the pyridazine N(3) nitrogen atoms, and to the S(1) sulphur atom of the coordinated dmso ligand.

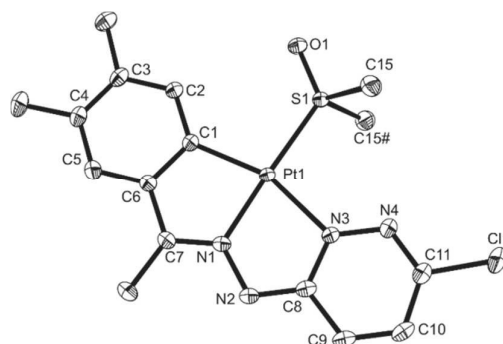


Figure 5. Molecular structure of $[\text{Pt}(3,4\text{-Me}_2\text{-C}_6\text{H}_2\text{C}(\text{Me})=\text{NN}(4'\text{-Cl-C}_4\text{H}_2\text{N}_2))\{(\text{CH}_3)_2\text{S}=\text{O}\}]$, **2e-dmso**. Hydrogen atoms have been omitted for clarity.

Bond distances and angles about the platinum atom are within the expected values.⁵⁹

π - π interactions, between the parallel pyridazine groups and the cyclometallated rings (separation distance of the ring centroids is 3.607(3) Å) were found.

The metal chelate rings [Pt(1), N(1), N(2), C(8), N(3)] of neighbouring molecules were also parallel and within the distance expected for a π - π "slipped stacking" interaction (separation between ring centroids 3.599(3) Å) (see Figure 6). The fact that we have previously observed similar interactions in an analogous complex with Pd(II) instead of Pt(II) as central atom 8 (see SI) is indicative that the intermolecular interactions do not depend on the metal atom.

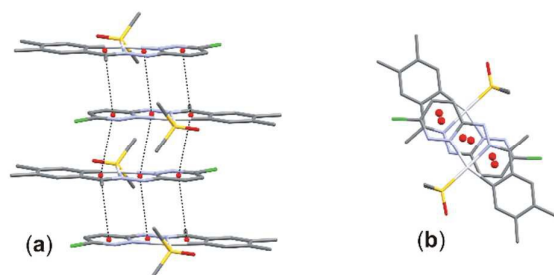


Figure 6. (a) view nearly perpendicular to *b* axis showing intermolecular π - π stacking interactions between molecules of $[\text{Pt}(3,4\text{-(Me)}_2\text{C}_6\text{H}_2\text{C(Me)=NN}(4'\text{-ClC}_6\text{H}_2\text{N}_2))][(\text{CH}_3)_2\text{S=O}]$, **2e-dmso**, dashed lines link the centroids of the rings involved in each stacking interaction. (b) View along *b* axis showing the antiparallel slipped stacking.

The molecules are stacked in an anti-parallel disposition that could be explained by the tendency of strongly polarized rings to adopt such disposition in order to maximize the dipole-dipole interactions.⁶⁰

In order to evaluate the energy of stacking interaction between the molecules in the crystal we decided to perform DFT calculations according to the method used by D. Zarić,¹⁷ using the TPSS-D3 functional with the def2-TZVP basis set and the counterpoise correction to eliminate the basis set superposition error. In particular, we performed the calculations over two stacked molecules of **2e-dmso** taken from the crystal structure without geometry optimization. At TPSS-D3/def2-TZVP level of theory, the counterpoise-corrected interaction energies calculated for **2e-dmso** and the palladium analogous were -25.05 and -22.94 kcal/mol, respectively. To gain further insight into the nature and origin of the stacking interactions, NCI index was computed for the crystal structure of **2e-dmso**.

Thus, NCI isosurfaces were obtained from promolecular densities calculated for an isolated molecule and a dimer formed by two stacked molecules within the crystal.^{43b} Figure 7(a) displays the computed NCI isosurfaces for the monomer, revealing repulsive interactions at the centre of the rings (red surfaces) and for the steric clashes of the methyl groups at the ligand (flat green-orange surfaces) as well as weak hydrogen bond-like attractive interactions involving the oxygen and the methyl groups of the dmso molecule (flat blue-green surfaces, for C-H2 \cdots O1 and C-H15 \cdots N4 contacts).^{43c} Figure 7(b) displays the NCI analysis computed for the dimer, which also includes a green sheet-like extended isosurface between the overlapping regions of the molecules, corresponding to the stacking interactions. Figures 7c and 7d only display the intermolecular interactions, with a shorter color scale to differentiate the attractive (bluish) from the repulsive (reddish) ones. The NCI analysis reveals the dispersion interactions between the Pt centre and C8-C9 moiety (at the pyridazine ring) and between N4-C10-C11 and C1-C6-C7 moieties (at pyridazine and cyclometallated rings, respectively) as the main attractive contributions to the delocalized π - π stacking interactions. The NCI peaks associated with these dispersion interactions appear at ρ values of -0.008 and -0.006 a.u., respectively (see SI,

Figure S4). In addition, intermolecular σ - σ dispersion interactions between methyl groups of hydrazone moiety and dmso (C-H14 \cdots H15-C, deep blue color) and hydrogen bond-like interactions between amine nitrogen and methyl group of dmso and between Cl and methyl group at hydrazone (C-H15 \cdots N2 and C-H14 \cdots Cl) are clearly visualized in the NCI analysis, and may contribute to strengthen the stacking interaction in the crystal structure.

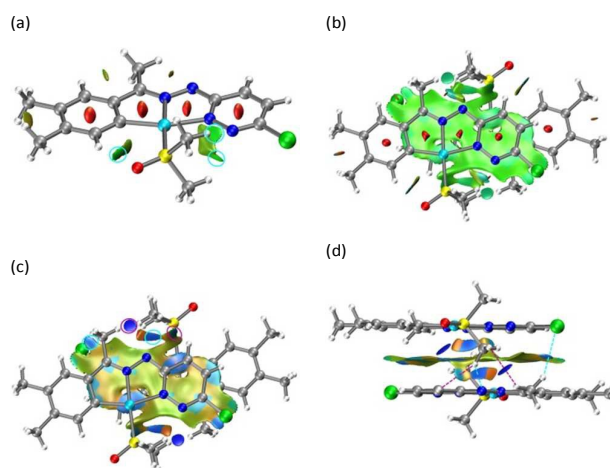


Figure 7. NCI analysis for the monomer and the dimer formed by two parallel molecules taken from crystal structure of **2e-dmso**. Gradient isosurfaces are colored on a BGR scale, according to the values of $\text{sign}(\lambda_2)\rho$: blue for attractive interaction, green for weak interaction and red for repulsive steric clashes. Region of weak hydrogen bond-like interactions highlighted in cyan, region of σ - σ dispersion interactions highlighted in magenta. (a) NCI isosurfaces for an isolated molecule with $s = 0.3$, color scale in the $-0.07 < \text{sign}(\lambda_2)\rho < 0.05$ au range. (b) NCI isosurfaces in the dimer with $s = 0.3$, color scale in the $-0.03 < \text{sign}(\lambda_2)\rho < 0.03$ au range. (c and d) Intermolecular NCI isosurfaces with $s = 0.3$, color scale in the shorter $-0.01 < \text{sign}(\lambda_2)\rho < 0.01$ au range, to highlight the attractive and repulsive dispersion interactions (b: view along the *b* axis, d: view near perpendicular to *b* axis).

Extended intramolecular isosurfaces as the one depicted in Figure 7, are characteristic of π - π stacked polycyclic aromatic systems such as naphthalene or anthracene.^{43b} In our case (Figure 7) the surface included the two metal chelate rings which could be indicative of the aromatic nature of such rings. Further evidence of metalloaromaticity was also supported on structural parameters according to Ghedini *et al*⁶¹ (see SI Figures S5 and S6).

In the molecular cation of **5e** each platinum atom is bonded, in a slightly distorted square-planar geometry to four atoms: one carbon atom of the phenyl ring and two nitrogen atoms, one from the C=N group and another from the heterocyclic ring. The fourth coordination position is occupied by one phosphorus atom from the $(\text{Ph}_2\text{PCH}_2\text{CH}_2)_2\text{PPh}$ (triphos) ligand which is acting as a bridging ligand binding three $[\text{Pt}(\text{C},\text{N},\text{N}')]$ moieties. All bond distances and angles are within the expected values.¹⁹

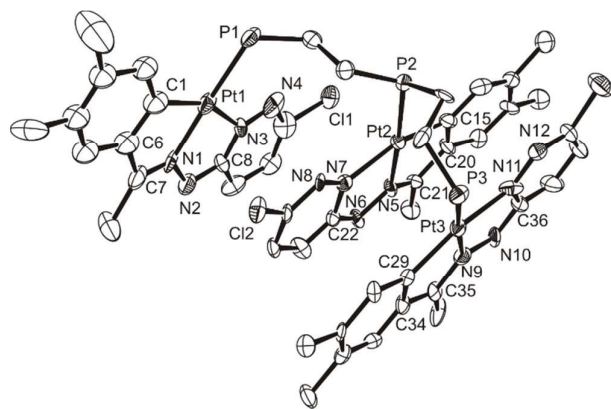


Figure 8. Molecular structure of the cation of **5e**. Hydrogen atoms and phosphine phenyl rings have been omitted for clarity reasons. Ellipsoids drawn at 40% of probability.

The cyclometallated moieties bonded to Pt(2) and Pt(3) adopt an almost anti-parallel disposition with a distance between the platinum atoms of 3.392(1) Å. This arrangement is stabilized by π - π stacking interactions between the metallated phenyls and the heterocyclic rings (distance between the ring centroids of approximately 3.4 Å) displaying the so-called “slipped stacking”. On the other hand, the centroid distances between the cyclometallated rings and the coordination rings are within the values expected for π - π stacked rings [3.264(8), and 3.271(9) Å]. This observation supports the existence of some degree of “metalloaromaticity” due to active charge delocalization (vide supra).

Similar “slipped stacking” π - π stacking interactions have also been found between the pyridazine rings bonded to Pt(1) and Pt(3), with a distance between the ring centroids of 3.503(9) Å (see Figure 9).

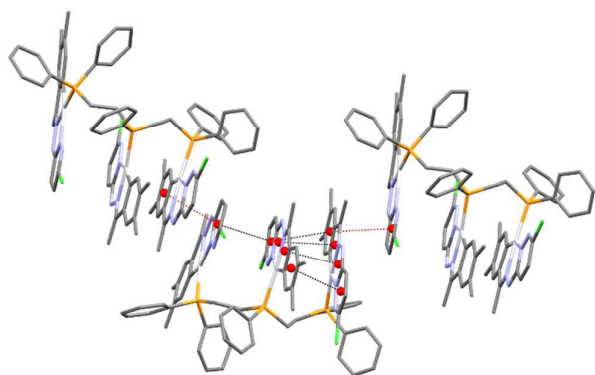


Figure 9. View of the intermolecular (in red) and intramolecular (in black) π - π stacking interactions within the crystal of **5e**, dashed lines link the centroids of the rings involved in each stacking interaction

Conclusions

Acetylpyridine *N*-phenylhydrazones react with $K_2[PtCl_4]$ in *n*-butanol/water at 100 °C showing a markedly different behaviour; the unsubstituted *N*-phenyl hydrazone (**b**) or the 3-

chloro substituted one (**c**) afforded directly cyclometallated complexes (**2b** and **2c**, respectively). Contrastingly, the reaction of the 2-chloro substituted *N*-phenyl hydrazone (**a**) or the 2,4-dichloro substituted one (**d**) under similar reaction conditions gave the non-cyclometallated complexes (**1a** and **1d**, respectively) regardless the reaction time. DFT studies have shown that cyclometallation takes place in three consecutive processes, involving initial iminoplatinum complex formation, followed by chelation and then final cycloplatination. With difference to related cycloplatinations which take place with liberation of methane,²⁸ lowest energy pathways for the cyclometallation of chelate complexes **1a,b** involves an electrophilic substitution pathway. DFT data indicate that formation of the intermediate chelate complexes **1a** and **1b** is thermodynamically favoured whilst cycloplatinations to **2a** and **2b** are calculated as endergonic processes. Hence, isolation of cyclometallated complex **2b** may only be explained if the hydrogen chloride formed as side-product is ionized and partially neutralized by the solvent mixture.^{44,45} However, under the same reaction conditions **2a** could not be prepared even though stabilization of the released HCl is also reasonable. Thus the reluctance of **1a** to experiment C-H activation may be explained in kinetic terms as a consequence of an increased activation energy for the nucleophilic attack of the *N*-phenyl moiety to the Pt(II) centre due to the presence of the electron withdrawing chlorine substituent. This increase in activation energy reduces the rate of cyclometallation in a sufficient extension to enable accumulation and isolation of the intermediate. The cyclometallation of **1a** to **2a** may be accomplished upon addition of NaOAc. The role of the acetate is dual; neutralizes the acidic media stabilizing the final products and enters the coordination sphere around the Pt(II) centre in the rate-determining step and facilitates subsequent hydrazone N-H deprotonation and electrophilic C-H activation.

On the other hand, reaction of ligand **e** derived from chloropyridazinhydrazone with $K_2[PtCl_4]$ in *n*-butanol/water at 100°C gave directly the cyclometallated complex **2e** with the imine group in the *endo* position. **2e** reacts with tertiary mono or triphosphines with or without opening of the coordination ring, depending on the denticity of the phosphine and the molar ration used. In dmsol solution **2e** exchanges the chloride ligand by a solvent molecule to give **2e-dmsol** which crystal structure showed π - π “slipped stacking” interaction with a separation between ring centroids of 3.599(3) Å. The NCI analyses seems to indicate that such interactions are probably due to the metalloaromatic nature of the chelate rings. Similar inter- and intramolecular interactions were also observed within the crystal of the trinuclear complex **5e** and in an analogue **8** to **2e-dmsol** with palladium instead of platinum as metal centre, indicating that such interactions might be ubiquitous among polycyclic complexes containing metal chelate rings.

Experimental

ARTICLE

Journal Name

A complete description of general methods, synthetic procedures, characterization details, computational methods and x-ray diffraction details are given in the SI.

General procedure for the cyclometallation of hydrazones with $K_2[PtCl_4]$: A pressure tube containing ligand **a-e** (4.07 mmol), $K_2[PtCl_4]$ (3.39 mmol) and 0.1 cm³ of water in 50 cm³ of 1-butanol was sealed under argon. The resulting mixture was stirred for 2-72 h at 100 °C. After cooling to room temperature the precipitate formed was filtered off, triturated with Et₂O and dried in vacuo.

General procedure for the acetate-assisted cycloplatination: A pressure tube containing chelated complex **1a,d** (0.195 mmol), NaOAc•3H₂O (0.195 mmol) and 50 cm³ of 1-butanol was sealed under argon. The resulting mixture was stirred for 24 h at 100 °C. After cooling to room temperature the brown precipitate formed was filtered off, triturated with Et₂O and dried in vacuo.

Typical procedure for the reaction of platinacycle **2e with phosphines:** PPh₃ (14 mg, 0.053 mmol) was added to a suspension of **2e** (28 mg, 0.055 mmol) in acetone (10 cm³). The mixture was stirred for 3 h and the solvent removed to give a red solid which was recrystallized from dichloromethane/ether.

Acknowledgements

We thank the Xunta de Galicia, Spain, for financial support (projects EM2014/056, PRGRC2014/042). The authors are indebted to Centro de Supercomputación de Galicia for providing the computer facilities.

Notes and references

- (a) I. Omae, *J. Organomet. Chem.*, 2007, **692**, 2608-2632; (b) M. López-Torres, A. Fernández, J. J. Fernández, S. Castro-Juiz, A. Suárez, J. M. Vila, M. T. Pereira, *Organometallics*, 2001, **20**, 1350-1353. (c) M. Marcos, *Metallomesogens. Synthesis, Properties and Applications*, J.L. Serrano (Ed.), VCH, Weinheim, 1996; (d) D. Pucci, G. Barneiro, A. Bellusci, A. Crispini, M. Ghedini, *J. Organomet. Chem.*, 2006, **691**, 1138-1142; (e) P. Espinet, M. A. Esteruelas, L. A. Oro, J. L. Serrano, E. Sola, *Coord. Chem. Rev.*, 1992, **17**, 215-274; (f) M. Ghedini, I. Aiello, A. Crispini, A. Golemme, M. La Deda, D. Pucci, *Coord. Chem. Rev.*, 2006, **250**, 1373-1390; (g) M. L. S. Lowry, S. Bernhard, *Chem. Eur. J.*, 2006, **12**, 7970-7977; (h) D.-L. Ma, V. P.-Y. Ma, D. S.-H. Chan, K.-H. Leung, H.-Z. He, C.-H. Leung, *Coord. Chem. Rev.*, 2012, **256**, 3087-3113. (i) J. M. Vila, M. T. Pereira, J. M. Ortigueira, J. J. Fernández, A. Fernández, M. López-Torres, H. Adams, *Organometallics*, 1999, **18**, 5484-5487.
- (a) I. Omae, *Organometallic Intramolecular-Coordination Compounds*, Elsevier Science, Amsterdam-New York, 1986; (b) V. V. Dunina, O. A. Zalevskaya, V. M. Potapov, *Russ. Chem. Rev.*, 1984, **571**, 250; (c) G. R. Newkome, W. E. Puckett, W. K. Gupta, G. E. Kiefer, *Chem. Rev.*, 1986, **86**, 451-489; (d) A. D. Ryabov, *Chem. Rev.*, 1990, **90**, 403-424; (e) M. Pfeffer, *Recl. Trav. Chim. Pyas-Bas*, 1990, **109**, 567-576; (f) J. Vicente, I. Saura-Llamas, *Comments Inorganic Chem.*, 2007, **28**, 39-72; (g) J. Dupont, C. S. Consorti, J. Spencer, *Chem. Rev.*, 2005, **105**, 2527-2572; (h) J. Djukic, A. Hijazi, H. D. Flack, G. Bernardinelli, *Chem. Soc. Rev.*, 2007, **37**, 406-425; (i) I. Omae, *Coord. Chem. Rev.*, 2004, **248**, 995-1023; (j) J. Dupont, M. Pfeffer, Eds., "Palladacycles", WILEY-VCH, Weinheim, 2008.
- (a) J. Kalinowski, V. Fattori, M. Cocchi, J. A. G. Williams, *Coord. Chem. Rev.*, 2011, **255**, 2401-2425; (b) V. Guerschais, J. Fillaut, *Coord. Chem. Rev.*, 2011, **255**, 2448-2457; (c) S. C. F. Kui, I. H. T. Sham, C. C. Cheung, C.-W. Ma, B. Pan, N. Zhu, C. M. Che, W.-F. Fu, *Chem. Eur. J.*, 2007, **13**, 417-435; (d) F. Gou, J. Cheng, X. Zhang, G. Shen, X. Zhou, H. Xiang, *Eur. J. Inorg. Chem.*, 2016, 4862-4866.
- (a) M. Fanelli, M. Formica, V. Fusi, L. Giorgi, M. Micheloni, P. Paoli, *Coord. Chem. Rev.*, 2016, **310**, 41-79; (b) A. Habtemariam, B. Watchman, B. S. Potter, R. Palmer, S. Parsons, A. Parkin, P. J. Sadler, *J. Chem. Soc. Dalton Trans.*, 2001, 1306-1318; (c) T. Okada, I.M. El-Mehasseb, M. Kodaka, T. Tomohiro, K. Okamoto, H. Okuno, *J. Med. Chem.*, 2001, **44**, 4661-4667; (d) J. Ruiz, J. Lorenzo, L. Sanglas, N. Cutillas, C. Vicente, M. D. Villa, F. X. Avilés, G. López, V. Moreno, J. Pérez, D. Bautista, *Inorg. Chem.*, 2006, **45**, 6347-6360; (e) C. Navarro-Ranninger, I. López-Solera, V. M. Gonzalez, J. M. Pérez, A. Alvarez-Valdés, A. Martín, P. R. Raithby, J. R. Masaguer, C. Alonso, *Inorg. Chem.*, 1996, **35**, 5181-5187; (f) N. Cutillas, G. S. Yellol, C. Haro, C. Vicente, *Coord. Chem. Rev.*, 2013, **257**, 2784-2797.
- (a) P. Chellan, K. M. Land, A. Shokar, A. Au, S. H. An, C. M. Clavel, P. J. Dyson, C. Kock, P. J. Smith, K. Chibale, G. S. Smith, *Organometallics*, 2012, **31**, 5791-5799; (b) J. M. Pérez, A. G. Quiroga, E. I. Montero, C. Alonso, C. Navarro-Ranninger, *J. Inorg. Biochem.*, 1999, **73**, 235-243.
- (a) J. M. Vila, M. Gayoso, M. T. Pereira, M. López-Torres, J. J. Fernández, A. Fernández, J. M. Ortigueira, *J. Organomet. Chem.*, 1997, **532**, 171-180; (b) J. M. Vila, M. T. Pereira, J. M. Ortigueira, D. Lata, M. López-Torres, J. J. Fernández, A. Fernández, H. Adams, *J. Organomet. Chem.*, 1998, **566**, 93-101; (c) A. Fernández, P. Uría, J. J. Fernández, M. López-

- Torres, A. Suárez, D. Vázquez-García, M. T. Pereira, J. M. Vila, *J. Organomet. Chem.*, 2001, **620**, 8-19; (d) A. Fernández, J. J. Fernández, M. López-Torres, A. Suárez, J. M. Ortigueira, J. M. Vila, H. Adams, *J. Organomet. Chem.*, 2000, **612**, 85-95; (e) M. López-Torres, A. Fernández, J. J. Fernández, A. Suárez, M. T. Pereira, J. M. Ortigueira, J. M. Vila, H. Adams, *Inorg. Chem.*, 2001, **40**, 4583-4587.
- 7 (a) J. Albert, J. Granell, J. Sales, X. Solans and M. Font-Altava *Organometallics*, 1986, **5**, 2567; (b) J. Albert, R. M. Ceder, M. Gomez J. Granell and J. Sales, *Organometallics*, 1992, **11**, 1536; (c) M. Gómez, J. Granell, M. Martinez, *J. Chem. Soc., Dalton Trans.*, 1998, 37-44; (d) M. Crespo, M. Font-Bardía, T. Calvet, *Dalton Trans.*, 2011, **40**, 9431-9438;
- 8 J. J. Fernández, A. Fernández, M. López-Torres, D. Vázquez-García, A. Rodríguez, A. Varela, J. M. Vila, *J. Organomet. Chem.*, 2009, **694**, 2234-2245.
- 9 A. Fernández, D. Vázquez-García, J. J. Fernández, M. López-Torres, A. Suárez, J. M. Vila, *J. Organomet. Chem.*, 2005, **690**, 3669-3679.
- 10 (a) G. García-Herbosa, A. Munoz, D. Miguel, S. Garcia-Granda, *Organometallics*, 1994, **13**, 1775-1780; (b) M. Ghedini, I. Aiello, A. Crispini, M. La Deda, *Dalton Trans.*, 2004, 1386-1392; (c) M. Nonoyama, C. Sugiura, *Polyhedron*, 1982, **1**, 179-181; (d) G. García-Herbosa, N. G. Connelly, A. Muñoz, J. V. Cuevas, A. G. Orpen, S. D. Politzer, *Organometallics*, 2001, **20**, 3223-3229; (e) M. S. Muñoz, B. García, S. Ibeas, F. J. Hoyuelos, I. Peñacobá, A. M. Navarro, J. M. Leal, *New J. Chem.*, 2004, **28**, 1450-1456; (f) I. Aiello, M. Ghedini, M. La Deda, T. Martino, *Inorg. Chem. Commun.* 2007, **10**, 825-828; (g) I. Aiello, M. Ghedini, M. La Deda, *J. Lumin.*, 2002, **96**, 249-259.
- 11 (a) D. J. Cárdenas, A. M. Echavarren, *Organometallics*, 1995, **14**, 4427-4430; (b) M. Nonoyama, C. Sugiura, *Polyhedron*, 1982, **1**, 179-181; (c) F. Ortega-Jiménez, J. G. López-Cortés, M. C. Ortega-Alfaro, A. Toscano, G. Penierres, R. Quijada, C. J. Alvarez, *Organomet. Chem.*, 2005, **690**, 454-462; (d) F. Ortega-Jiménez, E. Gómez, P. Sharma, M. C. Ortega-Alfaro, R. A. Toscano, C. Alvarez-Toledano, *Z. Anorg. Allg. Chem.*, 2002, **608**, 2104-2108; (e) J. Albert, A. González, J. Granell, R. Moragas, C. Puerta, P. Valerga, *Organometallics*, 1997, **16**, 3775-3778; (f) J. Albert, A. González, J. Granell, R. Moragas, X. Solans, M. J. Font-Bardía, *Chem. Soc. Dalton Trans.*, 1998, 1781-1785; (g) A. Rao, R. B. S. Pal, *J. Organomet. Chem.*, 2011, **696**, 2660-2664, 2012, **701**, 62-67 and 2013, **731**, 67-71.
- 12 For previous synthesis of cyclometallated complexes derived from hydrazones see, for example: (a) H. Sahebalzamani, S. Ghammamy, K. Mehrani, F. Salimi, N. M. Tarighi, *Asian Journal of Chemistry*, 2011, **23**, 26-28; (b) B. L. Shaw, S. D. Petrera, D. J. Shenton, M. Thornton-Pett, *Inorg. Chem. Acta*, 1998, **270**, 312-325; (c) M. B. Dinger, L. Main, B. K. Nicholson, *J. Organomet. Chem.*, 1998, **565**, 125-134; (d) N. Chitrapriya, V. Mahalingam, M. Zeller, K. Natarajan, *Polyhedron*, 2008, **27**, 1573-1580;
- 13 (a) M. Ghedini, I. Aiello, A. Crispini, M. La Deda, *Dalton Trans.*, 2004, 1386-1392; (b) K. Molčanov, M. Čurić, D. Babić, B. Kojić-Prodić, *J. Organomet. Chem.*, 2007, **692**, 3874-3879.
- 14 M. Ghedini, I. Aiello, A. Crispini, A. Golemme, M. La Deda, *Coord. Chem. Rev.*, 2006, **250**, 1373-1390.
- 15 (a) H. Masui, *Coord. Chem. Rev.*, 2001, **957**, 219-221; (b) M. K. Milčić, B. D. Ostojić, S. D. Zarić, *Inorganic Chemistry*, 2007, **46**, 7109-7114; (c) M. A. Iron, J. L. M. Martin, M. E. van der Boom, *J. Am. Chem. Soc.*, 2003, **125**, 11702-11709.
- 16 (a) Z. D. Tomić, D., Sredojević, S. D. Zarić, *Cryst. Growth Des.*, 2006, **6**, 29-31; (b) D. N. Sredojević, Z. D. Tomić, S. D. Zarić, *Cryst. Growth Des.*, 2010, **10**, 3901-3908; (c) Z. D. Tomić, S. B. Novaković, S. D. Zarić, *Eur. J. Inorg. Chem.*, 2004, 2215-2218; (d) D. N. Sredojević, Z. D. Tomić, S. D. Zarić, *Cent. Eur. J. Chem.*, 2007, **5**, 20-31; (e) D. P. Malenov, G. V. Janjić, V. B. Medaković, M. B. Hall, S. D. Zarić, *Coord. Chem. Rev.*, 2017, **345**, 318-341
- 17 P. V. Petrović, G. V. Janjić, S. D. Zarić, *Cryst. Growth Des.*, 2014, **14**, 3880-3889.
- 18 K. Ohno, M. Hasebe, A. Nagasawa, T. Fujihara, *Inorg. Chem.*, DOI: 10.1021/acs.inorgchem.7b014, and references therein.
- 19 (a) W. Lu, N. Zhu, C-M. Che, *Chem. Commun.*, 2002, 900-901; (b) W- Lu, M. C. W. Chan, N. Zhu, C. Che, C. Li, Z. Hui, *J. Am. Chem. Soc.*, 2004, **126**, 7639-7651; (c) P. Shao, W. Sun, *Inorg. Chem.*, 2007, **46**, 8603-8612.
- 20 (a) M. K. Raza, K. Mitra, A. Shettar, U. Basu, P. Kondaiah, A. R. Chakravarty, *Dalton Trans.*, 2016, **45**, 13234-13243; (b) C, R. Brodie, J. G. Collins, J. R. Aldrich-Wright, *Dalton Trans.*, 2004, 1145-1152; (c) B. J. Pages, J. Sakoff, J. Gilbert, A. Rodger, N. P. Chmel, N. C. Jones, S. M. Kelly, D. L. Ang, J. R. Aldrich-Wright, *Chem. Eur. J.*, 2016, **22**, 8943 - 8954.
- 21 J. M. Duff, B. E. Mann, B. L. Shaw, B. Turtle, *J. Chem. Soc., Dalton Trans.*, 1974, 139-145
- 22 (a) A. Gandioso, J. Valle-Sistac, L. Rodríguez, M. Crespo, M. Font-Bardía, *Organometallics*, 2014, **33**, 561-570; (b) A. Canapé, M. Crespo, J. Granell, M. Font-Bardía, X. Solans, *J. Organomet. Chem.*, 2005, **690**, 4309-4318; (c) A. Canapé, M. Crespo, J. Granell, M. Font-Bardía, X. Solans, *Dalton Trans.* 2003, 3763-3769.
- 23 (a) T. Calvet, M. Crespo, M. Font-Bardía, S. Jansat, M. Martínez, *Organometallics*, 2012, **31**, 4367-4373; (b) R. Martín, M. Crespo, M. Font-Bardía, T. Calvet, *Organometallics*, 2009, **28**, 587-597.
- 24 For reviews on computational studies on C-H bond activation by metal species, see: (a) D. Balcells, O. Eisenstein "Theoretical Studies on the Reaction Mechanism of Metal-Assisted C-H Activation" In *Comprehensive Inorganic Chemistry II*, Poeppelmeier, J. R., Ed., Elsevier: Amsterdam, 2013, Vol. 9, pp 695-726; (b) D. Balcells, E. Clot, O. Eisenstein, *Chem. Rev.*, 2010, **110**, 749-823; (c) Y. Boutadla,

- D. L. Davies, S. A. Macgregor, A. I. Poblador-Bahamonde, *Dalton Trans.*, 2009, 5820–5831. For a review on the mechanistic aspects of C-H activation by Pt complexes, see: M. Lersch, M. Tilset, *Chem. Rev.*, 2005, **105**, 2471–2526.
- 25 (a) Z. Xu, J. Oxgaard, W. A. Goddard, *Organometallics*, 2008, **27**, 3770–3773; (b) A. Paul, C. B. Musgrave, *Organometallics*, 2007, **26**, 793–809; (c) H. Zhu, T. Ziegler, *J. Organomet. Chem.*, 2006, **691**, 4486–4497; (d) X. Xu, J. Kua, R. A. Periana, W. A. Goddard III, *Organometallics*, 2003, **22**, 2057–2068; (e) J. Kua, X. Xu, R. A. Periana, W. A. Goddard III, *Organometallics*, 2002, **21**, 511–525; (f) T. M. Gilbert, J. Hristov, T. Ziegler, *Organometallics*, 2001, **20**, 1183–1189; (g) K. Mylvaganam, G. B. Bacskay, N. S. Hush, *J. Am. Chem. Soc.*, 2000, **122**, 2041–2052; (h) R. A. Periana, D. J. Taube, S. Gamble, H. Taube, T. Satoh, H. Fujii, *Science*, 1998, **280**, 560–564; (i) P. E. M. Siegbahn, R. H. Crabtree, *J. Am. Chem. Soc.*, 1996, **118**, 4442–4450.
- 26 (a) J.-L. Li, C.-Y. Geng, X.-R. Huang, X. Zhang, C.-C. Sun, *Organometallics*, 2007, **26**, 2203–2210; (b) V. R. Ziatdinov, J. Oxgaard, O. A. Mironov, K. J. H. Young, W. A. Goddard III, R. A. Periana, *J. Am. Chem. Soc.*, 2006, **128**, 7404–7405; (c) E. Khaskin, P. Y. Zavalij, A. N. Vedernikov, *J. Am. Chem. Soc.*, 2006, **128**, 13054–13055; (d) L. Johansson, O. B. Ryan, C. Romming, M. Tilset, *J. Am. Chem. Soc.*, 2001, **123**, 6579–6590.
- 27 (a) L. Maidich, G. Dettori, S. Stoccoro, M. A. Cinellu, J. P. Rourke, A. Zucca, *Organometallics*, 2015, **34**, 817–828; (b) B. Butschke, H. Schwarz, *Chem. Sci.*, 2012, **3**, 308–326.
- 28 (a) F. Julia, P. González-Herrero, *J. Am. Chem. Soc.*, 2016, **138**, 5276–5282; (b) M. Roselló-Merino, O. Rivada-Wheekaghan, M. A. Ortuño, P. Vidossich, J. Díez, A. Lledós, Conejero, S. Conejero, *Organometallics*, 2014, **33**, 3746–3756; (c) A. Marrone, N. Re, R. Romeo, *Organometallics*, 2008, **27**, 2215–2222; (d) B. Butschke, M. Schlangen, D. Schroder, H. Schwarz, *Chem. Eur. J.*, 2008, **14**, 11050–11060.
- 29 See, for instance: (a) D. Watts, D. Wang, M. Adelberg, P. I. Zavalij, A. N. Vedernikov *Organometallics* 2017, **36**, 207–219; (b) Y. Li, J. Carroll, B. Simpkins, D. Ravindranathan, C. M. Boyd, S. Huo, *Organometallics*, 2015, **34**, 3303–3313; (c) A. R. Balavardhana Rao, S. J. Pal, *Organomet. Chem.*, 2014, **762**, 58–66; (d) M. Albrecht, *Chem. Rev.*, 2010, **110**, 576–623 and references cited therein.
- 30 (a) The mechanism of benzo[h]quinolone cyclopalladation promoted by $[\text{PdCl}_4]^{2-}$ was studied by DFT methods, and the C-H activation has been predicted to proceed via deprotonation by internal or external base, see: X. Ke, T. R. Cundari, *Organometallics*, 2010, **29**, 821–834. (b) DFT calculations supporting the crystallographic evidences for the electrophilic nature of the cycloplatination of aryloximes with *cis*- $[\text{PtCl}_2(\text{dmsO})_2]$ has also been reported, see: S. Otto, A. Chanda, P. V. Samuleev, A. D. Ryabov, *Eur. J. Inorg. Chem.* 2006, 2561–2565.
- 31 Energetics for the dissociation of $[\text{PtCl}_4(\text{H}_2\text{O})_n]^{2-}$ into $[\text{PtCl}_3(\text{H}_2\text{O})_{n-2}]^-$ and $[\text{Cl}(\text{H}_2\text{O})_2]^-$ in vacuum have been reported, see: J. K. Park, B. G. Kim, *Bull. Korean Chem. Soc.*, 2006, **27**, 1405–1417. Equilibrium constants for species involved in aquation of $[\text{PtCl}_4]^{2-}$ have also been reported, see ref. 25c and references cited therein.
- 32 η_2 -(C,C) bonded arenes are commonly invoked as intermediates in C-H activation reactions, see ref. 26a for instance. Several Pt(II) arene complexes with η_2 -(C,C)-coordination mode have been structurally characterized by X-ray diffraction studies, see: (a) T. G. Driver, T. J. Williams, J. A. Labinger, J. E. Bercaw, *Organometallics*, 2007, **26**, 295–301; (b) J. R. Berenguer, J. Forníés, L. F. Martín, A. Martín, B. Menjón, *Inorg. Chem.*, 2005, **44**, 7265–7267; (c) C. A. Iverson, R. J. Lachicotte, C. Müller, W. D. Jones, *Organometallics*, 2002, **21**, 5320–5333; (d) S. Reinartz, P. S. White, M. Brookhart, J. L. Templeton, *J. Am. Chem. Soc.*, 2001, **123**, 12724–12725.
- 33 The reactions of $\text{K}[\text{PtCl}_3(\text{dmsO})]$ with ketimines and oximes have been shown to proceed at room temperature to yield the corresponding iminoplatinum(II) complexes, see (a) S. U. Pandya, K. C. Moss, M. R. Bryce, A. S. Batsanov, M. A. Fox, V. Janku, H. A. Al Attar, A. P. Monkman, *Eur. J. Inorg. Chem.*, 2010, 1963–1972; (b) Y. Y. Scaffidi-Domianello, A. A. Nazarov, M. Haukka, M. Galanski, B. K. Keppler, J. Schneider, P. Du, R. Eisenberg, V. Yu. Kukushkin, *Inorg. Chem.*, 2007, **46**, 4469–4482. Other platinum(II) Schiff base complexes have been obtained by using $\text{K}_2[\text{PtCl}_4]$, see: E. F. Reid, V. C. Cook, D. J. D. Wilson, C. F. Hogan, *Chem. Eur. J.*, 2013, **19**, 15907–15917 and references cited therein. Complexes of Zeise's salt $\text{K}[\text{Pt}(\text{C}_2\text{H}_4)\text{Cl}_3]$ with hydrazones in which the imino nitrogen acts as donor atom have been crystallographically characterized, see: L. Maresca, G. Natile, L. Cattalini, F. Gasparrini, *J. Chem. Soc. Dalton Trans.*, 1976, **12**, 1090–1093.
- 34 Initial dissociation of a dmsO ligand from *cis*- $[\text{PtCl}_2(\text{dmsO})_2]$ followed by endothermic coordination of benzylidene imine to the Pt(II) center has been proposed in the reaction path to seven-membered platinacycles with inserted arene systems, see: J. Albert, R. Bosque, M. Crespo, J. Granell, J. Rodríguez, J. Zafrilla, *Organometallics*, 2010, **29**, 4619–4627.
- 35 Reaction of *cis*- $[\text{PtCl}_2(\text{dmsO})_2]$ with aryloximes or guanidines afforded the corresponding iminoplatinum(II) complexes, which have been crystallographically characterized, see: (a) A. D. Ryabov, S. Otto, P. V. Samuleev, V. A. Polyakov, L. Alexandrova, G. M. Kazankov, S. Shova, M. Revenco, J. Lipkowski, M. H. Johansson, *Inorg. Chem.* 2002, **41**, 4286–4294; (b) P. Elumalai, N. Thirupathi, M. Nethaji *Inorg. Chem.* 2013, **52**, 1883–1894.
- 36 The energetics and reaction path in a series of $\text{S}_{\text{N}}2$ substitutions at square-planar Pt(II) complexes has been studied by DFT methods, see: J. Cooper, T. Ziegler, *Inorg. Chem.*, 2002, **41**, 6614–6622.

- 37 2-Pyridylhydrazone-diacetyl platinum(II) complexes have been crystallographically characterized, showing intramolecular hydrogen bonds, see: T. Kluge, E. Bette, M. Bette, J. Schmidt, D. Steinborn, *J. Organomet. Chem.*, 2014, **762**, 48-57.
- 38 The geometry of the agostic interaction calculated for intermediate **5b**⁺ is similar to that determined by single-crystal X-ray diffraction for a rhodium pincer complex (Rh-C 2.27 Å and Rh-H 1.95 Å), see: (a) A. Vigaloc, O. Uzan, L. J. W. Shimon, Y. Ben-David, J. M. L. Martin, D. Milstein, *J. Am. Chem. Soc.*, 1998, **120**, 12539-12544. For other complexes characterized by X-ray crystallography showing agostic interactions of aromatic C-H bonds, see: (b) A. C. Albeniz, G. Schulte, R. H. Crabtree, *Organometallics*, 1992, **11**, 242-249; (c) P. Dani, T. Karlen, R. A. Gossage, W. J. J. Smeets, A. L. Spek, G. van Koten, *J. Am. Chem. Soc.*, 1997, **119**, 11317-11318. For other T-shaped Pt(II) agostic complexes that have been crystallographically characterized see: (d) M. J. Ingleson, M. F. Mahon, A. S. Weller, *Chem. Commun.*, 2004, 2398-2399; (e) W. Baratta, S. Stoccoro, A. Doppiu, E. Herdtweck, A. Zucca, P. Rigo, *Angew. Chem. Int. Ed.*, 2003, **42**, 105-108.
- 39 The energy of an incipient agostic interaction in the *cis-trans* isomerization for cationic Pt(II) complexes was estimated by kinetic and computational data to be in the range of 5–8 kcal/mol: see R. Romeo, G. D'Amico, E. Sicilia, N. Russo, S. Rizzato, *J. Am. Chem. Soc.*, 2007, **129**, 5744–5755.
- 40 The activation energy for the electrophilic attack of the Pt(II) centre to the *N*-phenyl group on the chelate intermediate **1b** (32.8 kcal/mol) is lower than that calculated for the corresponding process on the mono-coordinate intermediate **4b**[−] (40.3 kcal/mol, see Supplementary Information, Scheme S9). Thus, chelation of the Pt(II) centre by the acetylpyridine hydrazone as a [N,N] bidentate ligand appears to facilitate the cyclometallation process.
- 41 DFT calculations for the initial steps of methane activation catalysed by [(HPzm)₂PtCl₄] or [(bpym)PtCl₂] revealed the involvement of associative transition structures and intermediate ion-pair methane complexes showing weak Pt-H interactions which resemble to transition structure *cis*-**1/5b** and ion-pair complex *cis*-**5b**, see ref 25a and ref 25e.
- 42 A. E. Reed, L. A. Curtiss, F. Weinhold, *Chem. Rev.*, 1988, **88**, 899–926.
- 43 The NCI method allows identification and visualization in real space of inter and intramolecular non-covalent interactions, based on the peaks that appear in the reduced density gradient (*s*) at low densities (*ρ*), see: (a) E. R. Johnson, S. Keinan, P. Mori-Sánchez, J. Contreras-García, A. J. Cohen, W. Yan, *J. Am. Chem. Soc.*, 2010, **132**, 6498-6506; (b) M. Alonso, T. Woller, F. J. Martín-Martínez, J. Contreras-García, P. Geerlings, F. De Proft, *Chem. Eur. J.*, 2014, **20**, 4931-4941; (c) R. Chaudret, B. de Courcy, J. Contreras-García, E. Gloaguen, A. Zehacker-Rentien, M. Mons, J.-P. Piquemal, *Phys. Chem. Chem. Phys.*, 2014, **16**, 9876-9891.
- 44 The ionization and neutralization of HCl in water are known to be exothermic processes, see: Handbook of Chemistry and Physics, 59th Ed., CRC Press: Boca Raton, FL, 1978. Calculation of the contribution of the ionization and neutralization of HCl in *n*-BuOH/H₂O to the energetic balance for the cyclometallation of **1a** to **2a** is beyond the scope of the present work. For recent progress in the theoretical determination of bond dissociation energies of small water and HCl clusters, see: A. K. Samanta, G. Czako, Y. Yang, J. S. Mancini, J. M. Bowman, H. Reisler, *Acc. Chem. Res.*, 2014, **47**, 2700-2709.
- 45 The increase in the reaction rate observed by the addition of water as solvent and the need to ionize HCl in cycloplatination reactions of diphenylpyridine using K₂[PtCl₄] has been reported, see: G. W. V. Cave, F. P. Fanizzi, R. J. Deeth, W. Errington, J. P. Rourke, *Organometallics*, 2000, **19**, 1355-1364.
- 46 One referee has suggested that the different reactivity observed for **1a** and **1b** might derive from the involvement of the chlorine substituent at the *N*-phenyl group in **1a** in a hydrogen bond with the hydrazine hydrogen. Nevertheless, such hydrogen bond-like interaction is present along the whole reaction coordinate in series **a**, and the calculated distances between the chlorine substituent and the hydrazine hydrogen for ligand **a**, intermediates **1a** and **5a**⁺, key transition structure **1/5a** and product **2a** are very similar (2.5-2.6 Å). Thus, there is not any computational evidence supporting the correlation between such hydrogen bond interaction and the increased activation energy for the nucleophilic attack of the *N*-(2-chlorophenyl) moiety to the Pt(II) centre.
- 47 M. Gómez, J. Granell, M. Martínez, *Organometallics*, 1997, **16**, 2539-2546.
- 48 (a) L. Ackermann, *Chem. Rev.*, 2011, **111**, 1315-1345. (b) J. Granell, M. Martínez, *Dalton Trans.* 2012, **41**, 11243–11258. For related palladium-catalyzed arylations, see: (c) S. I. Gorelsky, D. Lapointe, K. Fagnou, *J. Am. Chem. Soc.*, 2008, **130**, 10848; (d) D. Garcia-Cuadrado, P. de Mendoza, A. A. C. Braga, F. Maseras, A. M. Echavarren, *J. Am. Chem. Soc.*, 2007, **129**, 6880-6886.
- 49 For a recent review about computational studies of carboxylate-assisted C-H activation and functionalization at group 8-10 transition metal centers, see: D. L. Davies, S. A. Macgregor, C. L. McMullin, *Chem. Rev.* 2017, **117**, 8649-8709.
- 50 B. Biswas, M. Sugimoto, S. Sakaki, *Organometallics*, 2000, **19**, 3895-3908.
- 51 Computational studies by Davis *et al.* on cyclometallation reactions of dimethylbenzylamine with palladium or iridium precursors in the presence of stoichiometric amounts of

- acetate also indicated a two-step mechanism involving initial slow κ^2 - κ^1 displacement of acetate ligand and facile subsequent C-H activation *via* AMLA-6 transition structures, see: (a) D. L. Davies, S. M. A. Donald, S. A. Macgregor, *J. Am. Chem. Soc.* 2005, **127**, 13754-13755; (b) D. L. Davies, S. M. A. Donald, O. Al-Duaij, S. A. Macgregor, M. Pölleth, *J. Am. Chem. Soc.* 2006, **128**, 4210-4211.
- 52 Wheland intermediates were first invoked by Ryabov *et al.* to rationalize detailed kinetic and activation parameter measurements for the *ortho*-palladations of dimethylbenzylamine, see: A. D. Ryabov, I. K. Sakodinskaya, A. K Yatsimirsky, *J. Chem. Soc., Dalton Trans.* 1985, 2629-2638. Wheland-type intermediates have been characterized in cyclopalladations by DFT methods, see for example: A. J. Canty, A. Ariafard, B. F. Yates, M. S. Sanford, *Organometallics*, 2015, **34**, 1085-1090.
- 53 The number of well-characterized three-coordinate, 14-electron Pt(II) complexes is very low, due to the necessary blockage of the vacancy at the metal center to avoid intra- or intermolecular interactions such as agostic bonds, counteranions or solvent coordination that would mask the T-shaped structure (see ref. 44d and 44e). Nevertheless, coordinatively unsaturated Pt(II) species have been proposed as intermediates in numerous intramolecular C-H bond activations. For a review about true and masked T-shaped Pt(II) complexes, see: M. A. Ortuño, S. Conejero, A. Lledós, *Belstein J. Org. Chem.* 2013, **9**, 1352-1382.
- 54 The calculated mechanistic cycle for the alkoxylation of *N*-metoxybenzamides catalyzed by Pd(OAc)₂ in MeOH includes the coordination of Pd(II) acetate to the nitrogen followed by intramolecular proton transfer from the N-H group to acetate, also leading to an acetic acid bound intermediate, see: M. Anand, R. B. Sunoj, *Org. Lett.*, 2011, **13**, 4802-4805.
- 55 Acceleration of the cyclopalladation of imines by protonation of the abstracting ligand have been reported, see: J. Granell, M. Martínez, *Dalton Trans.*, 2012, **41**, 11243-11258.
- 56 Accordingly with this proposal, second-order perturbation theory analyses of Fock matrix in the NBO basis for **8ac** provided an estimated stabilization energy of 2.8 kcal/mol for the donor-acceptor interaction between a lone pair localized on the carbonyl oxygen and an empty lone pair on the coordinatively unsaturated Pt(II) centre. Moreover, the NCI surfaces calculated for **8ac** enabled the visualization of greenish forms around the Pt(II) centre, revealing attractive dispersion interactions with the acetic acid moiety and also with the chloride substituent at the phenyl ring (see SI, Figure S3A,B).
- 57 Wheland-type σ -complexes derived from Pt(II) and Pd(II) precursors have been crystallographically characterized, see: (a) K. Yamamoto, S. Kimura, T. Murahashi, *Angew. Chem, Int. Ed.* 2016, **55**, 5322-5326; (b) D. M. Grove, G. van Koten, J. N. Louwen, J. G. Noltes, A. L. Spek, H. J. C. Ubbels, *J. Am. Chem. Soc.*, 1982, **104**, 6609-6616.
- 58 In contrast, the molecular structure of the agostic intermediate **5a**⁺ showed a longer C-N(amine) bond (1.38 Å, analogous to that shown in the free ligand **a**), no appreciable puckering of the phenyl moiety, longer Pt-C bond length and stronger Pt-H contact (2.20 and 1.93 Å, respectively).
- 59 B. Cordero, V. Gómez, A. E. Platero-Prats, M. Revés, J. Echeverría, E. Cremades, F. Barragán, S. Alvarez, *Dalton Trans.*, 2008, 2832-2838.
- 60 C. Janiak, *J. Chem. Soc., Dalton Trans.*, 2000, 3885-3896.
- 61 A. Crispini, M. Ghedini, *J. Chem. Soc., Dalton Trans.*, 1997, 75-80.

Preparation and characterization of terdentate [C,N,N] acetophenone and acetylpyridine hydrazone platinumacyles. A DFT insight into the reaction mechanism

Ismael Marcos,^a Vicente Ojea,^a Digna Vázquez-García,^{a*} Jesús J. Fernández,^a Alberto Fernández,^a Margarita López-Torres,^a Jorge Lado^a and José M. Vila.^{b*}

Synthesis of Pt(II) organometallic complexes bearing tridentate hydrazones by direct and carboxylate-assisted C-H activation and mechanistic DFT studies.

